

ALTERNATIVE OXIDASE1a modulates the oxidative challenge during moderate Cd exposure in *Arabidopsis thaliana* leaves

Peer-reviewed author version

KEUNEN, Els; SCHELLINGEN, Kerim; Van Der Straeten, Dominique; REMANS, Tony; COLPAERT, Jan; VANGRONSVELD, Jaco & CUYPERS, Ann (2015)
ALTERNATIVE OXIDASE1a modulates the oxidative challenge during moderate Cd exposure in *Arabidopsis thaliana* leaves. In: JOURNAL OF EXPERIMENTAL BOTANY 66(10), p. 2967-2977.

DOI: 10.1093/jxb/erv035

Handle: <http://hdl.handle.net/1942/18494>

ALTERNATIVE OXIDASE1a modulates the oxidative challenge during moderate Cd exposure in *Arabidopsis thaliana* leaves

Short running title: AOX1a modulates the Cd-induced oxidative challenge

Els Keunen¹, Kerim Schellingen¹, Dominique Van Der Straeten², Tony Remans¹, Jan Colpaert¹, Jaco Vangronsveld¹ and Ann Cuypers^{1,*}

¹Environmental Biology, Centre for Environmental Sciences, Hasselt University, Agoralaan Building D, B-3590 Diepenbeek, Belgium

²Laboratory of Functional Plant Biology, Ghent University, Karel Lodewijk Ledeganckstraat 35, B-9000 Ghent, Belgium

Email addresses:

els.keunen@uhasselt.be

kerim.schellingen@uhasselt.be

dominique.vanderstraeten@ugent.be

tony.remans@uhasselt.be

jan.colpaert@uhasselt.be

jaco.vangronsveld@uhasselt.be

ann.cuypers@uhasselt.be

*Corresponding author: Ann Cuypers

Address:

Hasselt University - Campus Diepenbeek

Centre for Environmental Sciences

Agoralaan Building D

B-3590 Diepenbeek

Belgium

Telephone: +32-11268326

Fax: +32-11268299

Email: ann.cuypers@uhasselt.be

Date of submission: 21 November 2014

Number of Tables and Figures: 7 - Colour in print: Table 3, Fig. 2, Fig. 3 and Fig. 4

Total word count: 8271

Supplementary Data: 5 tables, 1 figure

Short statement

This study provides a working model for the involvement of the mitochondrial alternative oxidase 1a and its ethylene-dependent induction in plants under moderate Cd stress.

Abstract

This study aims to unravel the functional significance of alternative oxidase 1a (AOX1a) induction in cadmium (Cd)-exposed *Arabidopsis thaliana* leaves by comparing wild-type (WT) plants and *aox1a* knockout mutants. In the absence of AOX1a, differences in stress-responsive transcript and glutathione levels suggest an increased oxidative challenge during moderate (5 μ M) and prolonged (72 h) Cd exposure. Nevertheless, *aox1a* knockout leaves showed lower hydrogen peroxide (H₂O₂) accumulation as compared to the WT due to both acute (24 h) and prolonged (72 h) exposure to 5 but not 10 μ M Cd. Taken together, we propose a working model where AOX1a acts early in the response to Cd and activates or maintains a mitochondrial signalling pathway impacting on cellular antioxidative defence at post-transcriptional level. This fine-tuning pathway is suggested to function during moderate (5 μ M) Cd exposure while being overwhelmed during more severe (10 μ M) Cd stress. Within this framework, ethylene is required – either directly or indirectly via NADPH oxidase isoform C – to fully induce *AOX1* expression. In addition, a reciprocal crosstalk between these components was demonstrated in *A. thaliana* leaves under Cd exposure.

Keywords: alternative oxidase, alternative respiration, *Arabidopsis thaliana*, cadmium, ethylene, oxidative challenge.

Abbreviations: AOX, alternative oxidase; Cd, cadmium; ETC, electron transport chain; GSH, glutathione; GSSG, glutathione disulfide; H₂O₂, hydrogen peroxide; O₂^{•-}, superoxide; RBOH, respiratory burst oxidase homologue; ROS, reactive oxygen species.

67 **Introduction**

68 In the plant mitochondrial electron transport chain (ETC), two terminal oxidases are
69 able to reduce O₂ to H₂O. In contrast to cytochrome c oxidase (complex IV), the
70 alternative oxidase (AOX) does not translocate protons across the inner membrane.
71 As AOX bypasses proton-pumping complexes III and IV, the energy (ATP) yield is
72 reduced (Millar *et al.*, 2011). Under normal conditions, AOX is suggested to
73 modulate the production of reactive oxygen species (ROS), although conflicting
74 results appear in literature (Vanlerberghe *et al.*, 2009). Amirsadeghi *et al.* (2006)
75 have reported diminished steady-state cellular ROS levels in tobacco leaves lacking
76 AOX as compared to wild-type (WT) leaves. However, Cvetkovska and
77 Vanlerberghe (2012) evidenced that a lack of AOX increases superoxide (O₂^{•-}) levels
78 in tobacco leaf mitochondria. Nevertheless, these data support the long-standing
79 hypothesis that AOX modulates the production of mitochondrial ROS in plants
80 (Purvis and Shewfelt, 1993).

81 The relationship between ROS and AOX might also imply a function for this
82 enzyme during abiotic stress conditions, supported by the fact that expression of the
83 dominant *AOX1a* isoform in *Arabidopsis thaliana* is highly stress-responsive (Clifton
84 *et al.*, 2005; Vanlerberghe *et al.*, 2009). Abiotic stress is often characterised by an
85 oxidative challenge at the cellular and organellar level (Apel and Hirt, 2004). For
86 example, exposure to cadmium (Cd) is associated with increased ROS generation in
87 plants (Sharma and Dietz, 2009; Cuypers *et al.*, 2011) and mitochondria in particular
88 (Heyno *et al.*, 2008). Moreover, we reported that in case of Cd exposure, the AOX
89 pathway is activated at transcriptional and translational level in *A. thaliana* (Keunen
90 *et al.*, 2013). However, the functional implications of AOX induction during Cd
91 stress are still largely unknown.

92 Similarly to its function, it remains unclear how AOX is induced. Wang *et al.*
93 (2010) have shown that both hydrogen peroxide (H₂O₂) and ethylene are involved in
94 activating alternative respiration in salt-stressed *Arabidopsis* calli. Both ROS
95 (Cuypers *et al.*, 2011) and ethylene (Gallego *et al.*, 2012; Schellingen *et al.*, 2014)
96 are known to mediate Cd stress responses and therefore might also act in the
97 induction and activation of AOX during exposure to Cd.

98 The current study aims to unravel if and how AOX modulates Cd stress responses
99 in *A. thaliana*. To this end, we compared WT and *aox1a* knockout plants exposed to
100 sublethal Cd concentrations and monitored the Cd-induced oxidative challenge at the

101 transcript and metabolic level in leaves. Moreover, the emerging link between ROS,
102 ethylene and AOX induction and regulation was investigated through a combined
103 reverse genetic approach.
104

105 **Materials and methods**

106 *Plant culture and cadmium exposure*

107 Wild-type (WT), *aox1a* knockout (SALK_084897 T-DNA insertional line for
108 *AOX1a*; Alonso *et al.*, 2003; Watanabe *et al.*, 2008), ACC synthase (ACS)
109 *acs2-1/acs6-1* double knockout [N16581 NASC line, defective in Cd-induced
110 ethylene biosynthesis (Schellingen *et al.*, 2014)] and ethylene-insensitive *ein2-1* and
111 *ein2-5* (Alonso *et al.*, 1999) mutant genotypes were confirmed using PCR as
112 described in the above-mentioned papers. All seeds were surface-sterilised and
113 grown on hydroponics (Smeets *et al.*, 2008), except that purified sand was used
114 instead of rock wool (Keunen *et al.*, 2011). A modified Hoagland nutrient solution
115 was used (Smeets *et al.*, 2008) and growth conditions were set at a 12 h photoperiod,
116 65% relative humidity and day/night temperatures of 22 °C and 18 °C respectively.
117 Light was provided by Philips Green-Power LED modules. A combination of blue,
118 red and far-red modules was used to obtain a spectrum simulating the photosynthetic
119 active radiation (PAR) of sunlight. The PAR provided at the rosette level was 170
120 $\mu\text{mol m}^{-2} \text{s}^{-1}$. After 19 days of growth, plants were either exposed to 5 or 10 μM
121 CdSO_4 supplied to the roots or further grown under control conditions. After 24 and
122 72 h, leaf (entire rosette) samples were taken and the fresh weight was determined.
123 Samples were snap frozen in liquid nitrogen and stored at -70 °C for further analyses,
124 except for Cd content determination (cfr. *infra*; Keunen *et al.*, 2013).

125

126 *Determination of Cd content and dry weight*

127 At harvest, leaves were rinsed using distilled water. Samples were oven-dried and
128 weighed to determine the dry weight and the percentage of dry weight per plant,
129 calculated as the ratio between dry and fresh weight. Next, samples were digested
130 with 70-71% HNO_3 in a heat block (Cuypers *et al.*, 2002). Concentrations of Cd
131 were determined via inductively coupled plasma – optical emission spectrometry
132 (ICP-OES, Agilent Technologies, 700 Series, Belgium). For reference purposes,
133 blank (HNO_3 only) and standard [NIST Spinach (1570a)] samples were used.

134

135 *Gene expression analysis*

136 Frozen leaf samples were disrupted in 2 mL microcentrifuge tubes using two
137 stainless steel beads and the Retsch Mixer Mill MM 400 (Retsch, Belgium) under
138 frozen conditions. From the disrupted tissues, RNA was extracted using the

139 RNAqueous® Total RNA Isolation Kit (Ambion, Life Technologies, Belgium).
140 Concentration and purity of the isolated RNA were assessed using the NanoDrop®
141 ND-1000 spectrophotometer (ThermoScientific, USA). To remove any
142 contaminating genomic DNA, equal amounts (1 µg) of the extracted RNA samples
143 were subjected to a DNase treatment using the TURBO DNA-free™ Kit (Ambion).
144 Treated RNA samples were converted to single stranded cDNA via the
145 PrimeScript™ RT reagent Kit (Perfect Real Time, TaKaRa Bio Inc., Westburg, the
146 Netherlands). A tenfold dilution of the cDNA was made in 10⁻¹ diluted TE buffer
147 (1 mM Tris-HCl, 0.1 mM Na₂-EDTA, pH 8.0) and stored at -20 °C.

148 Quantitative real-time PCR was performed in optical 96-well plates using the
149 7500 Fast Real-Time PCR System (Applied Biosystems, Life Technologies,
150 Belgium) and the Fast SYBR® Green Master Mix (Applied Biosystems) according
151 to the manufacturer's instructions. Amplification occurred at universal cycling
152 conditions (20 s at 95°C, 40 cycles of 3 s at 95°C and 30 s at 60°C) followed by the
153 generation of a dissociation curve to verify amplification specificity. Gene-specific
154 forward and reverse primers (300 nM unless stated otherwise, Supplementary Table
155 S1) were designed and optimised via the Primer Express software (v2.0, Applied
156 Biosystems).

157 Gene expression levels were calculated via the 2^{-ΔC_q} method relative to the sample
158 with the highest expression (minimum C_q). All data were normalised to the
159 expression of three stable reference genes (Remans *et al.*, 2008) selected by geNorm
160 (v3.5; Vandesompele *et al.*, 2002) and Normfinder (v0.953; Andersen *et al.*, 2004)
161 algorithms. Data were normalised using the geometric average of the 2^{-ΔC_q} values for
162 *AT2G28390* (SAND family), *AT4G34270* (TIP41-like) and *AT5G25760* (UBC). All
163 details of our workflow according to the Minimum Information for publication of
164 Quantitative real-time PCR Experiments (MIQE) guidelines as described by Bustin
165 *et al.* (2009) are shown in Supplementary Table S2.

166

167 *Hierarchical clustering of gene expression data*

168 To identify potential sample-related patterns during Cd exposure in WT versus *aox1a*
169 knockout leaves, hierarchical clustering analysis was performed using GenEx
170 software (v6, MultiD Analyses AB, Sweden). This analysis was based on raw gene
171 expression values and the “Average linkage” algorithm, defining the distance
172 between groups/treatments as the average of distances between all pairs of

173 individuals in all groups. Distances between the measures were calculated via the
174 Euclidian Distance Measure. Heat maps were constructed to compare expression
175 levels between different genes and samples.

176

177 *In situ detection of H₂O₂ using 3,3'-diaminobenzidine*

178 Leaves were stained using 3,3'-diaminobenzidine (DAB) as described by Daudi *et al.*
179 (2012). After DAB oxidation by H₂O₂, an insoluble brown precipitate reflects the
180 presence and tissue distribution of H₂O₂. Leaves (three per plant, six biological
181 replicates per condition) were incubated in 3 mL freshly prepared staining solution
182 [DAB (1 mg mL⁻¹) and Tween-20 (0.05% v/v) in 10 mM Na₂HPO₄, pH 3.0] or
183 control solution (10 mM Na₂HPO₄) using 12-well microtiter plates. As DAB is
184 light-sensitive, all plates were covered using aluminium foil. To improve DAB
185 infiltration into the leaves, vacuum was applied during 5 min using a desiccator.
186 After shaking the plates at 80 rpm for 4 h, all solutions were replaced by 3 mL
187 bleaching solution (ethanol:acetic acid:glycerol; 3:1:1 v:v:v). After incubation at
188 95 °C during 15 min, the bleaching solution was refreshed, allowed to incubate at
189 room temperature for 30 min and finally stored at 4 °C. The following day, leaves
190 were observed under white light using a binocular microscope. Photographs were
191 obtained using a digital camera and BTV-pro software (Bensoftware). Experiments
192 were repeated twice using independent biological replicates and representative
193 pictures are depicted.

194

195 *Determination of glutathione content and redox state*

196 Contents of oxidised (GSSG) and reduced (GSH) forms of glutathione were
197 spectrophotometrically determined using the plate reader method previously
198 described by Queval and Noctor (2007). Frozen leaf samples (100 mg) were
199 thoroughly ground in liquid nitrogen using a cooled mortar and pestle. Sample
200 powders were homogenised in 200 mM HCl (800 µL per 120 mg fresh sample
201 weight) and centrifuged during 10 min (16 000g, 4 °C). Samples were adjusted to pH
202 4.5 and kept at 4 °C during the entire procedure unless specifically mentioned
203 otherwise. Measurement of GSH and GSSG is based on the reduction of
204 5,5-dithiobis(2-nitro-benzoic acid) (DTNB, 600 µM) by the action of glutathione
205 reductase (GR, 1U mL⁻¹) in the presence of NADPH (500 µM), which was
206 spectrophotometrically monitored at 412 nm during 5 min. Total glutathione

207 concentrations (GSH + GSSG) were calculated relative to a standard curve ranging
208 from 0 to 500 pmol GSH. To determine oxidised GSSG amounts, samples were first
209 incubated with 2-vinyl-pyridine (2-VP, 1% v/v) to precipitate all free GSH present in
210 the sample during 30 min at room temperature. Samples were centrifuged twice
211 (16 000g, 4 °C) to precipitate 2-VP prior to the measurement. For quantification
212 purposes, a GSSG standard curve ranging from 0 to 100 pmol was incubated with
213 2-VP and measured in duplicate concurrently with the samples. Reduced GSH
214 concentrations were derived by subtracting oxidised GSSG from total levels (Queval
215 and Noctor, 2007).

216

217 *Statistical analyses*

218 All datasets were statistically analysed with ANOVA and the Tukey-Kramer
219 post-hoc test to correct for multiple comparison using R version 2.13.1 (R
220 Development Core Team, 2011). Both normality and homoscedasticity were
221 checked; transformations were applied when necessary to approximate normality. If
222 normality could not be reached, a non-parametric Kruskal-Wallis test, followed by
223 the Wilcoxon rank sum test was used to determine statistical significance of the data.
224 Outliers were determined using the extreme studentised deviate analysis (GraphPad
225 Software, Inc.) at significance level 0.05. The statistical analysis used is indicated in
226 the caption of each Table or Figure.

227 For gene expression data, normalised relative quantities were log transformed
228 prior to statistical analysis (Supplementary Table S2). Both differences within and
229 between genotypes (Supplementary Table S3) and overall genotype * treatment
230 interaction effects (Supplementary Table S4) are discussed per time point.
231 Significant interaction effects depict genes where treatment (Cd) effects differ
232 between both genotypes.

233

234 **Results**

235 Responses of WT versus *aox1a* knockout plants were compared after 24 and 72 h of
236 exposure to 5 or 10 μ M Cd. Both concentrations were previously demonstrated to be
237 sublethal for the WT (Keunen *et al.*, 2011). The two time points were selected based
238 on our kinetic study in Cd-exposed WT plants, where *AOX1a* expression peaked
239 after 24 h and was still enhanced after 72 h Cd exposure in the leaves (Keunen *et al.*,
240 2013).

241

242 *Growth parameters and Cd uptake*

243 After 24 h, no significant changes in leaf fresh weight were observed for WT or
244 *aox1a* knockout plants (Table 1A and B). Significant decreases in fresh weight as
245 compared to leaves of unexposed plants were only apparent after 72 h of Cd
246 exposure in both genotypes (Table 1A and B). In general, changes in leaf fresh
247 weight were mirrored by the impact of Cd on dry weight (Table 1C) and dry weight
248 percentages (Table 1D) in a dose-dependent manner after 72 h in both genotypes.

249 The rise in Cd content in the leaves was correlated with the Cd concentration
250 applied to the nutrient solution, without any significant differences depending on the
251 genotype (Table 2).

252

253 *Connection between AOX1a and the Cd-induced oxidative challenge in A. thaliana* 254 *leaves*

255 When comparing WT and *aox1a* knockout plants, it is worthwhile to note that
256 transcript levels of all measured genes (except for *AOX1a*) did not differ between
257 unexposed genotypes. We previously demonstrated that sublethal Cd exposure
258 activates the mitochondrial alternative ETC at the transcript level in *A. thaliana* WT
259 leaves (Keunen *et al.*, 2013). In this research, it was demonstrated that only *AOX1a*
260 and *AOX1d* are expressed and increased upon Cd exposure in the leaves under our
261 experimental conditions. In the present study, *AOX1a* transcript levels significantly
262 peaked after 24 h exposure to both Cd concentrations in the WT (Fig. 1A). Without
263 functional *AOX1a*, transcript levels of *AOX1d* increased to a greater extent after
264 prolonged (72 h) exposure to 5 and 10 μ M Cd in the leaves as compared to the WT
265 (Fig. 1B).

266 Although genotype-dependent differences were observed for *AOX1a* and *AOX1d*
267 expression, Cd-induced changes in expression of alternative ETC components such

268 as alternative NAD(P)H dehydrogenases (NDs) and uncoupling proteins (UCPs)
269 (Keunen *et al.*, 2013) were generally similar in both WT and *aox1a* knockout leaves
270 (Supplementary Table S3). However, a significant overall genotype * treatment
271 interaction effect was observed for *UCP5* after 72 h (Supplementary Table S4),
272 indicating that the treatment effect differs between both genotypes. Indeed,
273 expression levels of this gene were higher in *aox1a* knockout than in WT leaves from
274 plants exposed to 5 μ M Cd during 72 h (Supplementary Table S3).

275 Gadjev *et al.* (2006) have described a set of five transcripts that were upregulated
276 more than fivefold in different experimental conditions eliciting oxidative stress.
277 These genes are now collectively referred to as hallmarks for general oxidative
278 stress, independent of the ROS type or where ROS are produced (Gadjev *et al.*,
279 2006). Transcript levels of all hallmark genes were increased in WT and *aox1a*
280 knockout plants upon Cd exposure (Fig. 1C-G). It should be noted however that
281 overall genotype * treatment interaction effects were significant for three markers
282 after 72 h (Supplementary Table S4). Transcript levels of the “upregulated by
283 oxidative stress” gene (*UPOX*, *AT2G21640*), expressed in plant mitochondria
284 (Sweetlove *et al.*, 2002), were used to estimate the extent of the mitochondrial
285 oxidative challenge induced by Cd. A clear genotype-dependent effect was detected
286 as *UPOX* expression was upregulated to a higher level after 72 h exposure to 5 μ M
287 Cd in *aox1a* knockout in comparison to WT leaves (Fig. 1C). Similar results were
288 obtained for the unknown *AT1G19020* (Fig. 1E) and TIR-class gene (*AT1G57630*,
289 Fig. 1G).

290 To further characterise the Cd-induced oxidative challenge at the metabolic level,
291 H₂O₂ production and glutathione (GSH) concentrations and redox state were
292 determined. In both genotypes, Cd exposure increased the presence of DAB
293 precipitates after 24 and 72 h (Fig. 2). However, the leaves of *aox1a* knockout plants
294 exposed to 5 μ M Cd showed less intense staining as compared to WT plants (Fig. 2,
295 middle row panels), suggesting a lower production of H₂O₂ under these conditions.
296 Concerning the concentrations and redox state of GSH (Table 3), a markedly lower
297 GSSG content was observed for WT and *aox1a* knockout plants after 24 h exposure
298 to 5 or 10 μ M Cd as compared to control conditions. Consequently, a more reduced
299 redox state was apparent (Table 3). After 72 h, GSSG levels rose at 10 μ M Cd,
300 however only significantly in *aox1a* knockout mutants, but without significant
301 alteration of the redox state (Table 3). Reduced and total GSH levels significantly

302 increased in 5 μ M Cd-exposed WT plants after 72 h. This was not observed in *aox1a*
303 knockout mutants (Table 3). However, exposure to 10 μ M Cd caused similar
304 increases in GSH levels in both WT and *aox1a* knockout leaves (Table 3).

305

306 *Transcriptional alterations in ROS producing and scavenging components*

307 Exposure to Cd affects transcript levels of genes encoding ROS producing and
308 scavenging proteins (Cuypers *et al.*, 2011; Jozefczak *et al.*, 2014). In this study, our
309 aim was to determine if and how AOX1a affects the Cd-induced oxidative challenge
310 at the transcript level in *A. thaliana* leaves. Therefore, relative expression levels of
311 different ROS producing, both mitochondrial and other ROS scavenging genes
312 (Supplementary Table S1) were determined in WT and *aox1a* knockout plants
313 exposed to 5 or 10 μ M Cd during 24 and 72 h (Supplementary Tables S3 and S4). In
314 general, for WT plants, responses corresponded with our earlier work as described by
315 Cuypers *et al.* (2011), Keunen *et al.* (2013) and Jozefczak *et al.* (2014). Expression
316 levels of ROS producing lipoxxygenases and antioxidative genes such as catalase
317 isoforms 1 and 3 and glutathione reductase 1 were increased after Cd exposure.
318 Moreover, the Cd-mediated decrease in copper/zinc superoxide dismutase expression
319 was confirmed (Supplementary Table S3). When comparing WT and *aox1a*
320 knockout plants, it is worthwhile to note that transcript levels of all measured genes
321 did not differ between unexposed genotypes. Although Cd-induced expression
322 changes were generally similar in both genotypes, a significant genotype * treatment
323 interaction effect was observed for the respiratory burst oxidase homologue C
324 (*RBOHC*) gene after prolonged (72 h) Cd exposure (Supplementary Table S4).
325 Indeed, *RBOHC* expression levels increased to a greater extent in *aox1a* knockout as
326 compared to WT plants after 72 h exposure to 5 μ M Cd (Supplementary Table S3).

327 Hierarchical clustering analysis including all samples and all measured genes
328 (Supplementary Table S1) was performed for both genotypes (Fig. 3). Control
329 samples clustered apart from Cd-exposed samples in WT as well as *aox1a* mutant
330 plants. In WT leaves, Cd-exposed samples were generally grouped per time point (24
331 and 72 h) independent of the Cd concentration applied (Fig. 3A). While the same
332 held true for Cd-exposed samples after 24 h in *aox1a* knockout mutants, a separate
333 clustering of 5 and 10 μ M Cd-exposed samples occurred after 72 h in the absence of
334 AOX1a (Fig. 3B).

335

336 *Mechanistic insights into AOX induction and regulation in leaves of Cd-exposed*
337 *A. thaliana plants*

338 Ethylene is undoubtedly involved in Cd-induced signalling as recently evidenced by
339 Schellingen *et al.* (2014). Moreover, ethylene and/or ROS are potentially involved in
340 modulating AOX upregulation during stress (Wang *et al.*, 2010; Li *et al.*, 2013). To
341 further strengthen the emerging link between ethylene, ROS and AOX, we used a
342 reverse genetic approach combining ethylene biosynthesis (*acs2-1/6-1* knockout),
343 ethylene signalling (*ein2-1*) and *aox1a* knockout mutants. Based on the increased
344 induction of the oxidative stress hallmark genes in leaves of 5 μ M Cd-exposed *aox1a*
345 knockout as compared to WT plants, all genotypes were exposed to 5 μ M Cd during
346 24 and 72 h. Transcript levels were compared between different genotypes and
347 expressed relatively to their own control (Fig. 4). Under control conditions,
348 expression levels of *AOX1a*, *AOX1d* and *RBOHC* were significantly higher in *ein2-1*
349 mutants as compared to the WT, albeit only after 24 h (Supplementary Table S5).
350 Upregulation of *AOX1a* (Fig. 4A) and *AOX1d* (Fig. 4B) was significantly lower in
351 leaves of both ethylene mutants exposed to 5 μ M Cd as compared to WT plants.
352 Moreover, *RBOHC* upregulation was weaker or even absent in Cd-exposed
353 *acs2-1/6-1* and *ein2-1* mutants (Fig. 4C). Similar results were obtained for the leaves
354 of 5 μ M Cd-exposed *ein2-5* mutants (Supplementary Fig. S1).

355 After 72 h exposure to 5 μ M Cd, transcript levels of *RBOHC* were higher in
356 *aox1a* knockout leaves as compared to the WT (Fig. 4D). Similarly, expression of
357 the ethylene biosynthesis ACC synthase 6 (*ACS6*, Fig. 4E) and the ethylene receptor
358 2 (*ETR2*, Fig. 4F) gene was induced to a greater extent under the same conditions.
359 Both observations point towards a regulatory role of *AOX1a* in the upregulation of
360 *RBOHC* and genes involved in ethylene synthesis and signalling (middle scheme in
361 Fig. 4). For the sake of completeness, transcript levels of ethylene biosynthesis as
362 well as signal transduction genes (Supplementary Table S1) were determined in WT
363 and *aox1a* knockout plants, also after exposure to 10 μ M Cd (Supplementary Table
364 S3). In general, most differences observed between both genotypes after prolonged
365 (72 h) exposure to 5 μ M Cd (Fig. 4) disappeared after exposure to the highest Cd
366 concentration (Supplementary Table S3).

367

368

369

370 Discussion

371 Previous results indicated that AOX respiration is involved in *A. thaliana* stress
372 responses to Cd at transcript and protein level (Keunen *et al.*, 2013). In the current
373 work, we studied the significance of AOX induction during moderate (5 μ M) and
374 more severe (10 μ M) Cd stress by comparing WT and *aox1a* knockout plants. Prior
375 to Cd exposure, no clear phenotypic differences were visible between both
376 genotypes. Corresponding with previous research (Giraud *et al.*, 2008), this supports
377 the view that a lack of AOX has minor to no consequences under non-stress
378 conditions but particularly impacts (abiotic) stress responses (Vanlerberghe *et al.*,
379 2009). However, Cd content and weight parameters were comparably affected in WT
380 and *aox1a* knockout plants (Tables 1 and 2). Therefore, Cd-induced responses were
381 compared between both genotypes at the molecular level.

382

383 *A modulating role for AOX1a during the oxidative challenge under moderate (5 μ M)* 384 *Cd exposure*

385 In general, our assessment of the Cd-induced oxidative challenge at transcript and
386 metabolic level revealed that most differences between WT and *aox1a* knockout
387 plants were occurring under moderate *i.e.* 5 μ M Cd exposure. For example,
388 expression levels of the oxidative stress hallmark genes *UPOX* (Fig. 1C),
389 *AT1G19020* (Fig. 1E) and the TIR-class gene (Fig. 1G) were induced to a higher
390 extent after 72 h exposure to 5 μ M Cd in *aox1a* knockout in comparison to WT
391 leaves. As demonstrated by Cvetkovska and Vanlerberghe (2012), a lack of AOX
392 increases mitochondrial $O_2^{\bullet-}$ production. Therefore, higher *UPOX* upregulation in
393 the absence of AOX1a coincides with an enhanced mitochondrial oxidative
394 challenge under moderate Cd stress. Moreover, a lack of functional AOX1a can have
395 consequences outside mitochondria, as evidenced by the higher upregulation of the
396 chloroplast TIR-class gene in leaves of 5 μ M Cd-exposed *aox1a* knockout versus
397 WT plants. Similarly, Giraud *et al.* (2008) reported increases in stress-responsive
398 transcripts and particularly those that encode ROS scavengers in chloroplasts during
399 combined light and drought stress in the absence of AOX1a.

400 Under normal conditions, it has been shown that AOX-suppressed tobacco leaves
401 have similar to lower H_2O_2 concentrations as compared to WT leaves (Cvetkovska
402 and Vanlerberghe, 2012). Consistently, results in both tobacco (Amirsadeghi *et al.*,
403 2006) and *Arabidopsis* (Watanabe *et al.*, 2008) point towards induced ROS

404 scavenging when AOX is missing. Nevertheless, we did not observe differences in
405 DAB staining between WT and *aox1a* knockout leaves under normal growth
406 conditions. During exposure to 5 μ M Cd however, H₂O₂ accumulated to a lesser
407 extent in *aox1a* knockout leaves (Fig. 2). Pasqualini *et al.* (2007) reported that leaves
408 of transgenic tobacco plants overexpressing AOX1a showed increased and persistent
409 H₂O₂ levels during acute ozone fumigation as compared to WT plants. The
410 attenuation of H₂O₂ levels after 24 and 72 h of Cd exposure in our study could have
411 an impact at a more prolonged stage (72 h), for example when comparing GSH
412 responses in both genotypes. The absence of a significant increase in GSH levels in
413 leaves of 5 μ M Cd-exposed *aox1a* knockout as compared to WT plants after 72 h
414 (Table 3) coincides with an altered oxidative challenge as evidenced by the hallmark
415 genes (Fig. 1).

416 Taken together, our data suggest that a lack of functional AOX1a disrupts a
417 signalling pathway emerging from the mitochondrion early after the start of Cd
418 exposure. A role for AOX1a in acute Cd stress responses is underlined by the
419 observed peak in its expression levels after 24 h (Fig. 1A) and its transient increase at
420 the protein level (Keunen *et al.*, 2013). The nature of the retrograde signal initiated
421 by AOX is currently unknown, but ROS are often put forward (Vanlerberghe *et al.*,
422 2009). In line with this, we suggest the involvement of H₂O₂ as its levels were
423 attenuated in leaves of plants lacking AOX1a during 5 μ M Cd exposure.
424 Nevertheless, the role of other signalling metabolites should also be explored as
425 AOX is intimately related to the carbon and nitrogen metabolism under physiological
426 (Gandin *et al.*, 2014) and stress conditions (Watanabe *et al.*, 2008). In addition, it is
427 unclear which cellular functional level is controlled by the AOX1a signalling
428 pathway during Cd stress. Expression levels of genes involved in the ROS network
429 did not change in leaves of *aox1a* knockout versus WT plants (Supplementary Table
430 S3). Therefore, we suggest the AOX1a signalling pathway to regulate defence
431 mechanisms to moderate (5 μ M) Cd stress at a post-transcriptional level in
432 *A. thaliana* leaves.

433 In reverse genetic studies, it is often observed that other components of the
434 alternative respiratory pathway such as NDs and UCPs try to compensate for the
435 absence of functional AOX1a. For example, Watanabe *et al.* (2008) have
436 demonstrated increased transcript levels of *NDB2* and *UCP1* isoforms in *A. thaliana*
437 leaves lacking AOX1a as compared to the WT under low temperature. While in our

study *ND* and *UCP* genes mostly did not show altered expression levels in the absence of AOX1a (Supplementary Table S3), expression of *AOX1d* was more abundant in leaves of Cd-exposed *aox1a* knockout mutants, again highly pronounced after 72 h exposure to 5 μ M Cd (Fig. 1B). Strödtkotter *et al.* (2009) have demonstrated that AOX1d was unable to take over the function of AOX1a in *A. thaliana* exposed to antimycin A. Functional compensation of AOX1a by AOX1d is unlikely in our conditions as well, since *aox1a* knockout mutants did show a differential response to 5 μ M Cd as compared to WT plants.

Finally, all differences observed in leaves of 5 μ M Cd-exposed *aox1a* knockout as compared to WT plants after 72 h disappeared when comparing responses to the highest Cd concentration. This is supported by our clustering analysis, where leaf samples from 5 μ M Cd-exposed mutants clustered separately from those derived from plants exposed to 10 μ M Cd at 72 h (Fig. 3). The latter plants severely suffer as indicated by approximately 50% growth inhibition (Table 1B) and increased total H₂O₂ levels (Fig. 2). The enhanced ROS accumulation did cause oxidative damage, but only after 72 h exposure to the highest Cd concentration (Keunen *et al.*, 2013). Therefore, we hypothesise the AOX1a signal to initiate a fine-tuning pathway that is overwhelmed when stress levels are more severe (10 μ M Cd). Nonetheless, plants are able to survive long-term exposure to 10 μ M Cd (Keunen *et al.*, 2011).

The emerging link between ethylene, ROS and AOX in leaves of Cd-exposed A. thaliana plants

Recently, more research is dedicated to unravelling the nature of primary signals that genetically control AOX respiration in plants (Vanlerberghe, 2013). Li *et al.* (2013) have shown that mitochondrial O₂^{•−} modulates rice *AOX1* gene expression under cold, drought and salinity stress. In addition to ROS, ethylene was shown to be implicated in the induction of alternative respiration in salt-treated *Arabidopsis* calli (Wang *et al.*, 2010).

In the current work, we demonstrate the necessity of functional ethylene biosynthesis and signal transduction to fully induce *AOX1* genes in leaves of 5 μ M Cd-exposed *A. thaliana* plants (Fig. 4). To this end, we compared transcriptional responses in Cd-exposed WT and *acs2-1/6-1* knockout plants. The use of these mutants is justified as increased expression levels of both ACS2 and ACS6 mainly mediate ethylene biosynthesis and responses in Cd-exposed *A. thaliana* plants

472 (Schellingen *et al.*, 2014). In *acs2-1/6-1* knockout mutant leaves, induction of both
473 *AOX1a* and *AOX1d* was lowered as compared to the WT, most pronounced after
474 24 h exposure to 5 μ M Cd. Furthermore, Cd-induced responses were compared
475 between WT plants and *ein2-1* mutants. As EIN2 is a central component in the
476 ethylene signalling pathway, *ein2-1* mutant lines are completely insensitive to this
477 hormone (Alonso *et al.*, 1999). Under ethylene insensitive conditions, the induction
478 of *AOX1a* and *AOX1d* by Cd completely disappeared after 72 h (Fig. 4A and B). A
479 similar response was observed for *ein2-5* mutants as compared to the WT
480 (Supplementary Fig. S1). A link between ethylene and *AOX1d* induction was also
481 reported by Buchanan-Wollaston *et al.* (2005), who observed diminished
482 upregulation of *AOX1d* in senescing leaves of *ein2-1* mutants as compared to WT
483 plants. Furthermore, AOX was demonstrated to play a regulatory role during
484 ethylene-induced plant cell death (Lei *et al.*, 2003) as well as tomato fruit ripening
485 (Xu *et al.*, 2012). Exposure to Cd is related to accelerated leaf ageing (Sandalio *et*
486 *al.*, 2001) and ethylene might at least contribute to this response in *A. thaliana*
487 (Schellingen *et al.*, 2014).

488 Although ethylene induces *AOX1* expression during Cd exposure, also other
489 components are suggested to be involved. Ederli *et al.* (2006) showed that both
490 ethylene-dependent and -independent pathways are required to increase *AOX1a*
491 expression in tobacco plants exposed to ozone. In addition, evidence was presented
492 for the essential role of nitric oxide (NO) as upstream signalling component
493 activating AOX. As NO is suggested to be involved in Cd stress responses as well
494 (Arasimowicz-Jelonek *et al.*, 2011), its role in genetic control of AOX respiration
495 should be addressed in future studies.

496 It is tempting to speculate about the involvement of ROS and more particularly
497 $O_2^{\bullet-}$ generated by NADPH oxidases (dashed arrows in Fig. 4) in the modulation of
498 AOX by ethylene. Jiang *et al.* (2013) have demonstrated that enhanced ethylene
499 production potently promotes salt tolerance in *A. thaliana*, which is correlated with
500 elevated ROS levels and RBOHF function. Moreover, expression of *RBOHD* and
501 *RBOHF* genes is preceded by ethylene biosynthesis in *Brassica oleracea*
502 (Jakubowicz *et al.*, 2010). Upon Cd exposure, expression of *RBOHC* that was the
503 highest induced isoform in leaves (Remans *et al.*, 2010) did not increase to WT
504 levels in *acs2-1/6-1* knockout, *ein2-1* (Fig. 4C) and *ein2-5* mutants (Supplementary
505 Fig. S1). These results clearly link ethylene to ROS production by NADPH oxidases,

506 which might also mediate stress responses inducing *AOX1* genes and leading to
507 signalling and acclimation during moderate *i.e.* 5 μ M Cd exposure. On the other
508 hand, the involvement of negative feedback mechanisms from AOX to
509 RBOHC/ethylene was demonstrated using *aox1a* knockout plants. Indeed, the
510 induction of *RBOHC* (Fig. 4D), the ethylene biosynthesis gene *ACS6* (Fig. 4E) and
511 ethylene signalling gene *ETR2* (Fig. 4F) was enhanced in the absence of AOX1a.
512 This higher induction correlates with an increased expression level of the oxidative
513 stress hallmark genes in leaves of 5 μ M Cd-exposed *aox1a* knockout as compared to
514 WT plants after 72 h (Fig. 1). Taken together, these data suggest a reciprocal
515 crosstalk between ethylene, RBOHC and AOX during moderate Cd exposure in
516 *A. thaliana* leaves (Fig. 4).
517

518 **Supplementary Data**

519

520 **Supplementary Table S1.** Forward (FW) and reverse (REV) primers used to
521 determine gene expression levels via quantitative real-time PCR.

522

523 **Supplementary Table S2.** Quantitative real-time PCR parameters according to the
524 Minimum Information for publication of Quantitative real-time PCR Experiments
525 (MIQE) guidelines derived from Bustin *et al.* (2009).

526

527 **Supplementary Table S3.** Relative leaf transcript levels of wild-type and *aox1a*
528 knockout *Arabidopsis thaliana* plants.

529

530 **Supplementary Table S4.** Overall genotype * treatment interaction effects
531 represented by the p-values for all measured genes in wild-type and *aox1a* knockout
532 *Arabidopsis thaliana* leaves per time point.

533

534 **Supplementary Table S5.** Relative leaf transcript levels of genes encoding
535 alternative oxidases (*AOX1a* and *AOX1d*) and respiratory burst oxidase homologue c
536 (*RBOHC*) in different genotypes of *Arabidopsis thaliana* under control conditions.

537

538 **Supplementary Fig. S1.** Relative leaf transcript levels of alternative oxidases
539 *AOX1a* (A), *AOX1d* (B) and respiratory burst oxidase homologue C (C) in wild-type
540 and *ein2-5* mutant *Arabidopsis thaliana* plants.

541

542 **Funding**

543 This work was supported by the Research Foundation Flanders (FWO) by a PhD
544 grant for EK and the project [G0D3414]. Additional funding came from Hasselt
545 University through the Methusalem project [08M03VGRJ].

546

547 **Acknowledgments**

548 We thank Carine Put and Ann Wijgaerts for their skilful technical assistance. Seeds
549 of *aox1a* knockout plants (Columbia ecotype) were kindly provided by Dr. Chihiro
550 Watanabe (Department of Biological Sciences, Graduate School of Science, The
551 University of Tokyo, Japan).

References

- Andersen CL, Jensen JL, Ørntoft TF.** 2004. Normalization of real-time quantitative reverse transcription-PCR data: A model-based variance estimation approach to identify genes suited for normalization, applied to bladder and colon cancer data sets. *Cancer Research* **64**, 5245–5250.
- Alonso JM, Hirayama T, Roman G, Nourizadeh S, Ecker JR.** 1999. EIN2, a bifunctional transducer of ethylene and stress responses in *Arabidopsis*. *Science* **284**, 2148–2152.
- Alonso JM, Stepanova AN, Leisse TJ, et al.** 2003. Genome-wide insertional mutagenesis of *Arabidopsis thaliana*. *Science* **301**, 653–657.
- Amirsadeghi S, Robson CA, McDonald AE, Vanlerberghe GC.** 2006. Changes in plant mitochondrial electron transport alter cellular levels of reactive oxygen species and susceptibility to cell death signaling molecules. *Plant and Cell Physiology* **47**, 1509–1519.
- Apel K, Hirt H.** 2004. Reactive oxygen species: Metabolism, oxidative stress, and signal transduction. *Annual Review of Plant Biology* **55**, 373–399.
- Arasimowicz-Jelonek M, Floryszak-Wieczorek J, Gwóźdź EA.** 2011. The message of nitric oxide in cadmium challenged plants. *Plant Science* **181**, 612–620.
- Buchanan-Wollaston V, Page T, Harrison E, et al.** 2005. Comparative transcriptome analysis reveals significant differences in gene expression and signalling pathways between developmental and dark/starvation-induced senescence in *Arabidopsis*. *The Plant Journal* **42**, 567–585.
- Bustin SA, Benes V, Garson JA, et al.** 2009. The MIQE guidelines: Minimum Information for publication of Quantitative real-time PCR Experiments. *Clinical Chemistry* **55**, 611–622.
- Clifton R, Lister R, Parker KL, Sappl PG, Elhafez D, Millar AH, Day DA, Whelan J.** 2005. Stress-induced co-expression of alternative respiratory chain components in *Arabidopsis thaliana*. *Plant Molecular Biology* **58**, 193–212.
- Cuypers A, Vangronsveld J, Clijsters H.** 2002. Peroxidases in roots and primary leaves of *Phaseolus vulgaris*. Copper and zinc phytotoxicity: a comparison. *Journal of Plant Physiology* **159**, 869–876.
- Cuypers A, Smeets K, Ruytinx J, et al.** 2011. The cellular redox state as a modulator in cadmium and copper responses in *Arabidopsis thaliana* seedlings. *Journal of Plant Physiology* **168**, 309–316.

- Cvetkovska M, Vanlerberghe GC.** 2012. Alternative oxidase modulates leaf mitochondrial concentrations of superoxide and nitric oxide. *New Phytologist* **195**, 32–39.
- Daudi A, Cheng Z, O'Brien JA, Mammarella N, Khan S, Ausubel FM, Bolwell GP.** 2012. The apoplastic oxidative burst peroxidase in *Arabidopsis* is a major component of pattern-triggered immunity. *The Plant Cell* **24**, 275–287.
- Ederli L, Morettini R, Borgogni A, Wasternack C, Miersch O, Reale L, Ferranti F, Tosti N, Pasqualini S.** 2006. Interaction between nitric oxide and ethylene in the induction of alternative oxidase in ozone-treated tobacco plants. *Plant Physiology* **142**, 595–608.
- Gadjev I, Vanderauwera S, Gechev TS, Laloi C, Minkov IN, Shulaev V, Apel K, Inzé D, Mittler R, Van Breusegem F.** 2006. Transcriptomic footprints disclose specificity of reactive oxygen species signaling in *Arabidopsis*. *Plant Physiology* **141**, 436–445.
- Gallego SM, Pena LB, Barcia RA, Azpilicueta CE, Iannone MF, Rosales EP, Zawoznik MS, Groppa MD, Benavides MP.** 2012. Unravelling cadmium toxicity and tolerance in plants: Insight into regulatory mechanisms. *Environmental and Experimental Botany* **83**, 33–46.
- Gandin A, Denysyuk M, Cousins AB.** 2014. Disruption of the mitochondrial alternative oxidase (AOX) and uncoupling protein (UCP) alters rates of foliar nitrate and carbon assimilation in *Arabidopsis thaliana*. *Journal of Experimental Botany* **65**, 3133–3142.
- Giraud E, Ho LHM, Clifton R, et al.** 2008. The absence of ALTERNATIVE OXIDASE1a in *Arabidopsis* results in acute sensitivity to combined light and drought stress. *Plant Physiology* **147**, 595–610.
- Heyno E, Klose C, Krieger-Liszkay A.** 2008. Origin of cadmium-induced reactive oxygen species production: mitochondrial electron transfer versus plasma membrane NADPH oxidase. *New Phytologist* **179**, 687–699.
- Jakubowicz M, Galgańska H, Nowak W, Sadowski J.** 2010. Exogenously induced expression of ethylene biosynthesis, ethylene perception, phospholipase D, and Rboh-oxidase genes in broccoli seedlings. *Journal of Experimental Botany* **61**, 3475–3491.

- Jiang C, Belfield EJ, Cao Y, Smith JAC, Harberd NP.** 2013. An *Arabidopsis* soil-salinity-tolerance mutation confers ethylene-mediated enhancement of sodium/potassium homeostasis. *The Plant Cell* **25**, 3535–3552.
- Jozefczak M, Keunen E, Schat H, Blik M, Hernández LE, Carleer R, Remans T, Bohler S, Vangronsveld J, Cuypers A.** 2014. Differential response of *Arabidopsis* leaves and roots to cadmium: Glutathione-related chelating capacity vs antioxidant capacity. *Plant Physiology and Biochemistry* **83**, 1–9.
- Keunen E, Truyens S, Bruckers L, Remans T, Vangronsveld J, Cuypers A.** 2011. Survival of Cd-exposed *Arabidopsis thaliana*: are these plants reproductively challenged? *Plant Physiology and Biochemistry* **49**, 1084–1091.
- Keunen E, Jozefczak M, Remans T, Vangronsveld J, Cuypers A.** 2013. Alternative respiration as a primary defence during cadmium-induced mitochondrial oxidative challenge in *Arabidopsis thaliana*. *Environmental and Experimental Botany* **91**, 63–73.
- Lei XY, Zhu RY, Zhang GY, Dai YR.** 2003. Possible involvement of the mitochondrial alternative pathway in ethylene-induced apoptosis in tomato protoplasts. *Plant Growth Regulation* **41**, 111–116.
- Li CR, Liang DD, Li J, Duan YB, Li H, Yang YC, Qin RY, Li L, Wei PC, Yang JB.** 2013. Unravelling mitochondrial retrograde regulation in the abiotic stress induction of rice *ALTERNATIVE OXIDASE 1* genes. *Plant, Cell and Environment* **36**, 775–788.
- Millar AH, Whelan J, Soole KL, Day DA.** 2011. Organization and regulation of mitochondrial respiration in plants. *Annual Review of Plant Biology* **62**, 79–104.
- Pasqualini S, Paolocci F, Borgogni A, Morettini R, Ederli L.** 2007. The overexpression of an alternative oxidase gene triggers ozone sensitivity in tobacco plants. *Plant, Cell and Environment* **30**, 1545–1556.
- Purvis AC, Shewfelt RL.** 1993. Does the alternative pathway ameliorate chilling injury in sensitive plant tissues? *Physiologia Plantarum* **88**, 712–718.
- Queval G, Noctor G.** 2007. A plate reader method for the measurement of NAD, NADP, glutathione, and ascorbate in tissue extracts: Application to redox profiling during *Arabidopsis* rosette development. *Analytical Biochemistry* **363**, 58–69.
- R Development Core Team.** 2011. R: A language and environment for statistical computing. R Foundation for Statistical Computing, Vienna, Austria. ISBN 3-900051-07-0, URL <http://www.R-project.org/>.

- Remans T, Smeets K, Opdenakker K, Mathijsen D, Vangronsveld J, Cuypers A.** 2008. Normalisation of real-time RT-PCR gene expression measurements in *Arabidopsis thaliana* exposed to increased metal concentrations. *Planta* **227**, 1343–1349.
- Remans T, Opdenakker K, Smeets K, Mathijsen D, Vangronsveld J, Cuypers A.** 2010. Metal-specific and NADPH oxidase dependent changes in lipoxygenase and NADPH oxidase gene expression in *Arabidopsis thaliana* exposed to cadmium or excess copper. *Functional Plant Biology* **37**, 532–544.
- Sandalio LM, Dalurzo HC, Gómez M, Romero-Puertas MC, del Río LA.** 2001. Cadmium-induced changes in the growth and oxidative metabolism of pea plants. *Journal of Experimental Botany* **52**, 2115–2126.
- Schellingen K, Van Der Straeten D, Vandenbussche F, Prinsen E, Remans T, Vangronsveld J, Cuypers A.** 2014. Cadmium-induced ethylene production and responses in *Arabidopsis thaliana* rely on ACS2 and ACS6 gene expression. *BMC Plant Biology* **14**, 214.
- Sharma SS, Dietz KJ.** 2009. The relationship between metal toxicity and cellular redox imbalance. *Trends in Plant Science* **14**, 43–50.
- Smeets K, Ruytinx J, Van Belleghem F, Semane B, Lin D, Vangronsveld J, Cuypers A.** 2008. Critical evaluation and statistical validation of a hydroponic culture system for *Arabidopsis thaliana*. *Plant Physiology and Biochemistry* **46**, 212–218.
- Strodtkötter I, Padmasree K, Dinakar C, et al.** 2009. Induction of the AOX1D isoform of alternative oxidase in *A. thaliana* T-DNA insertion lines lacking isoform AOX1A is insufficient to optimize photosynthesis when treated with antimycin A. *Molecular Plant* **2**, 284–297.
- Sweetlove LJ, Heazlewood JL, Herald V, Holtzapffel R, Day DA, Leaver CJ, Millar AH.** 2002. The impact of oxidative stress on *Arabidopsis* mitochondria. *The Plant Journal* **32**, 891–904.
- Vandesompele J, De Preter K, Pattyn F, Poppe B, Van Roy N, De Paepe A, Speleman F.** 2002. Accurate normalization of real-time quantitative RT-PCR data by geometric averaging of multiple internal control genes. *Genome Biology* **3**, research0034.1–034.11.

- Vanlerberghe GC, Cvetkovska M, Wang J.** 2009. Is the maintenance of homeostatic mitochondrial signaling during stress a physiological role for alternative oxidase? *Physiologia Plantarum* **137**, 392–406.
- Vanlerberghe GC.** 2013. Alternative oxidase: A mitochondrial respiratory pathway to maintain metabolic and signaling homeostasis during abiotic and biotic stress in plants. *International Journal of Molecular Sciences* **14**, 6805–6847.
- Wang H, Liang X, Huang J, Zhang D, Lu H, Liu Z, Bi Y.** 2010. Involvement of ethylene and hydrogen peroxide in induction of alternative respiratory pathway in salt-treated *Arabidopsis* calluses. *Plant and Cell Physiology* **51**, 1754–1765.
- Watanabe CK, Hachiya T, Terashima I, Noguchi K.** 2008. The lack of alternative oxidase at low temperature leads to a disruption of the balance in carbon and nitrogen metabolism, and to an up-regulation of antioxidant defence systems in *Arabidopsis thaliana* leaves. *Plant, Cell and Environment* **31**, 1190–1202.
- Xu F, Yuan S, Zhang DW, Lv X, Lin HH.** 2012. The role of alternative oxidase in tomato fruit ripening and its regulatory interaction with ethylene. *Journal of Experimental Botany* **63**, 5705–5716.

Tables

Table 1. Weight parameters of leaves harvested from wild-type (WT) and *aox1a* knockout (*aox1a*) *Arabidopsis thaliana* plants. All parameters were determined for 19-days-old plants exposed to 5 or 10 μM CdSO_4 during 24 and 72 h or grown under control conditions. Data are given as the mean \pm S.E. of five biological replicates, each consisting of at least ten individual rosettes. (A) Fresh weight expressed in mg per plant. (B) The percentage of growth inhibition relative to the control (0.00%). (C) Dry weight expressed in mg per plant. (D) Percentage dry weight per plant. Different letters represent significant differences within and between both genotypes ($p < 0.05$), tested within each exposure time (two-way ANOVA).

	24 h		72 h	
	WT	<i>aox1a</i>	WT	<i>aox1a</i>
A. Fresh weight (mg)				
Control	60.08 \pm 2.31a	55.12 \pm 2.97a	100.84 \pm 2.94a	89.98 \pm 4.64a
5 μM Cd	57.20 \pm 2.62a	55.70 \pm 0.72a	73.45 \pm 4.28b	67.06 \pm 3.01b,d
10 μM Cd	54.30 \pm 2.76a	56.36 \pm 1.84a	46.93 \pm 3.22c	52.69 \pm 2.48c,d
B. Growth inhibition relative to control (%)				
Control	0.00a	0.00a	0.00a	0.00a
5 μM Cd	4.79a	0.00a	27.16b,d	25.47b
10 μM Cd	9.61a	0.00a	53.46c	41.44c,d
C. Dry weight (mg)				
Control	5.38 \pm 0.27a	4.87 \pm 0.25a	8.80 \pm 0.24a	7.86 \pm 0.41a,b
5 μM Cd	5.33 \pm 0.18a	5.18 \pm 0.06a	7.92 \pm 0.35a,b	7.28 \pm 0.22a,b
10 μM Cd	5.35 \pm 0.31a	5.55 \pm 0.22a	6.55 \pm 0.49b	7.19 \pm 0.39b
D. Dry weight (%)				
Control	8.95 \pm 0.12a	8.85 \pm 0.13a	8.73 \pm 0.08a	8.74 \pm 0.07a
5 μM Cd	9.35 \pm 0.18a,b	9.30 \pm 0.09a,b	10.82 \pm 0.36b	10.90 \pm 0.32b
10 μM Cd	9.83 \pm 0.11b	9.85 \pm 0.12b	13.99 \pm 0.60c	13.68 \pm 0.58c

Table 2. Cadmium content (mg kg^{-1} dry weight) of leaves harvested from wild-type (WT) and *aox1a* knockout (*aox1a*) *Arabidopsis thaliana* plants. Cadmium levels were determined in 19-days-old plants exposed to 5 or 10 μM CdSO_4 during 24 and 72 h or grown under control conditions. Data are given as the mean \pm S.E. of five biological replicates. No Cd could be detected in unexposed plants (nd). Different letters represent significant differences within and between both genotypes ($p < 0.05$), tested within each exposure time (two-way ANOVA).

	24 h		72 h	
	WT	<i>aox1a</i>	WT	<i>aox1a</i>
Control	nd	nd	nd	nd
5 μM Cd	799.25 \pm 47.01a	803.66 \pm 24.94a	1440.93 \pm 78.58a	1578.63 \pm 61.63a
10 μM Cd	1441.17 \pm 115.12b	1284.11 \pm 117.28b	2027.68 \pm 138.17b	2273.63 \pm 106.61b

Table 3. Leaf glutathione (GSH) concentrations (nmol GSH equivalents g⁻¹ fresh weight) and redox state. Total GSH levels consist of both reduced (GSH) and oxidised glutathione disulfide (GSSG), thereby also determining the ratio between oxidised and reduced forms *i.e.* the redox state. Concentrations were determined in leaves of 19-days-old wild-type (WT) and *aox1a* knockout (*aox1a*) *Arabidopsis thaliana* plants exposed to 5 or 10 µM CdSO₄ during 24 and 72 h or grown under control conditions. Data are given as the mean ± S.E. of at least four biological replicates. Per time point, significant Cd-induced changes within a genotype are indicated with colour shading: $p < 0.05$; $p < 0.01$ and $p < 0.05$; $p < 0.01$ for increases and decreases respectively (one-way ANOVA).

		24 h		72 h	
		WT	<i>aox1a</i>	WT	<i>aox1a</i>
Total GSH + GSSG	Control	223.53 ± 12.86	210.48 ± 15.78	171.03 ± 9.31	173.22 ± 5.82
	5 µM Cd	194.31 ± 25.34	201.80 ± 13.37	312.34 ± 25.31	254.95 ± 29.83
	10 µM Cd	257.82 ± 15.06	218.30 ± 16.92	397.90 ± 43.90	456.04 ± 36.92
GSH	Control	216.76 ± 13.10	197.37 ± 15.33	162.39 ± 9.50	166.03 ± 5.98
	5 µM Cd	193.51 ± 25.39	197.47 ± 12.04	305.14 ± 24.42	246.69 ± 30.30
	10 µM Cd	255.14 ± 14.50	213.39 ± 17.01	381.01 ± 43.94	445.86 ± 36.00
GSSG	Control	6.77 ± 1.60	13.10 ± 1.51	8.64 ± 1.41	5.15 ± 0.65
	5 µM Cd	0.80 ± 0.11	0.94 ± 0.20	7.20 ± 1.66	8.26 ± 1.13
	10 µM Cd	2.68 ± 1.22	4.91 ± 1.02	16.89 ± 4.41	10.18 ± 1.31
GSSG / GSH	Control	0.032 ± 0.008	0.067 ± 0.008	0.054 ± 0.010	0.031 ± 0.005
	5 µM Cd	0.005 ± 0.001	0.005 ± 0.001	0.023 ± 0.005	0.037 ± 0.008
	10 µM Cd	0.010 ± 0.005	0.024 ± 0.006	0.048 ± 0.013	0.023 ± 0.002

Figure legends

Fig. 1. Relative leaf transcript levels of *AOX1a* (A), *AOX1d* (B) and the oxidative stress hallmark genes (C-G) in *Arabidopsis thaliana*. Transcript levels were measured via quantitative real-time PCR in leaf samples of 19-days-old wild-type (WT) and *aox1a* knockout (*aox1a*) plants exposed to 5 μ M (WT: white; *aox1a*: white striped) or 10 μ M (WT: grey; *aox1a*: grey striped) CdSO₄ during 24 and 72 h or grown under control conditions. Per time point, data are given as the mean \pm S.E. of four biological replicates relative to the unexposed genotype set at 1.00 (dashed line). Within each genotype and time point, significant Cd-induced expression changes relative to the control are indicated using asterisks: ** $p < 0.01$. Different letters denote significant differences within and between both genotypes ($p < 0.05$), tested within each exposure time (two-way ANOVA). *AOX*, alternative oxidase; *UPOX*, upregulated by oxidative stress; *TIR*, Toll-Interleukin-1.

Fig. 2. Hydrogen peroxide (H₂O₂) production as detected by 3,3'-diaminobenzidine (DAB) in the leaves. Staining was performed using leaves of wild-type (WT) and *aox1a* knockout (*aox1a*) *Arabidopsis thaliana* plants either exposed to 5 or 10 μ M CdSO₄ during 24 and 72 h or grown under control conditions. Per condition, three rosette leaves of six biological replicates were sampled, and representative photographs from two independent experiments are depicted here.

Fig. 3. Hierarchical classification of transcript levels in leaf samples. Results are visualised using dendrograms and heat maps indicating expression levels in the leaves of wild-type (A) and *aox1a* knockout (B) *Arabidopsis thaliana* plants. Each column of the map represents a different gene.

Fig. 4. Schematic overview of the interplay between ethylene, RBOHC and AOX in leaves of Cd-exposed *Arabidopsis thaliana* plants. Transcript levels were measured via quantitative real-time PCR in leaf samples of 19-days-old wild-type (WT) plants and *acs2-1/acs6-1* double knockout (*acs2-1/6-1*), ethylene-insensitive *ein2-1* or *aox1a* knockout mutants (*aox1a*) exposed to 5 μ M CdSO₄ (WT: white; mutant: white striped) during 24 and 72 h or grown under control conditions. Per time point, data are given as the mean \pm S.E. of four biological replicates relative to the unexposed

genotype set at 1.00 (dashed line). Within each genotype and time point, significant Cd-induced expression changes relative to the control are indicated using asterisks: * $p < 0.05$, ** $p < 0.01$. Different letters denote significant differences between both genotypes ($p < 0.05$), tested within each exposure time (two-way ANOVA). Expression levels of *AOX1a* (A), *AOX1d* (B) and *RBOHC* (C) were determined in WT, *acs2-1/6-1* and *ein2-1* mutants. Moreover, *RBOHC* (D), *ACS6* (E) and *ETR2* (F) transcript levels were measured in WT and *aox1a* mutants. A working model for the putative interactions between ethylene, RBOHC and AOX is depicted in the middle. ACS, ACC synthase; AOX, alternative oxidase; ETR, ethylene receptor; RBOHC, respiratory burst oxidase homologue C.

Figures

Fig. 1.

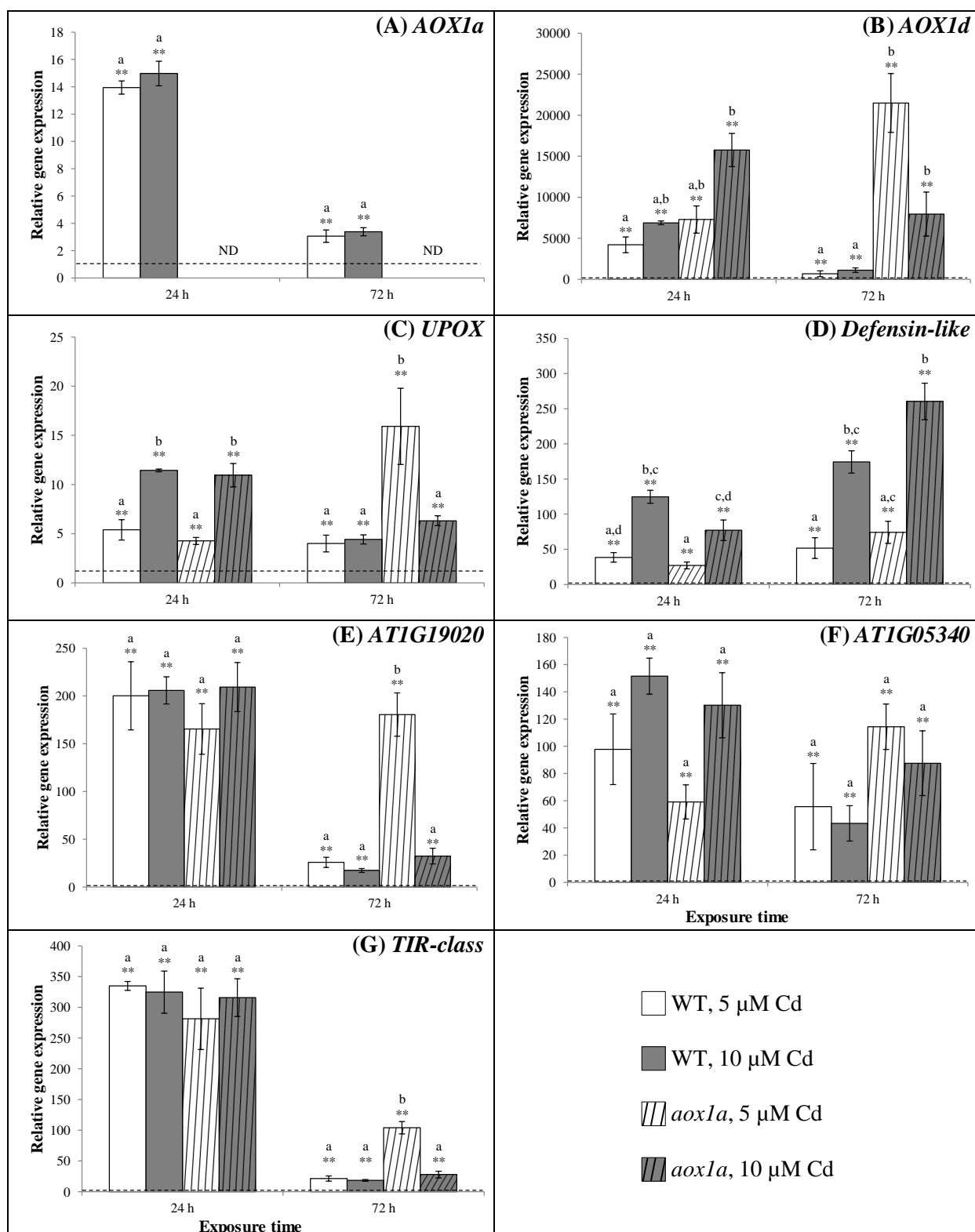


Fig. 1. (TIFF)

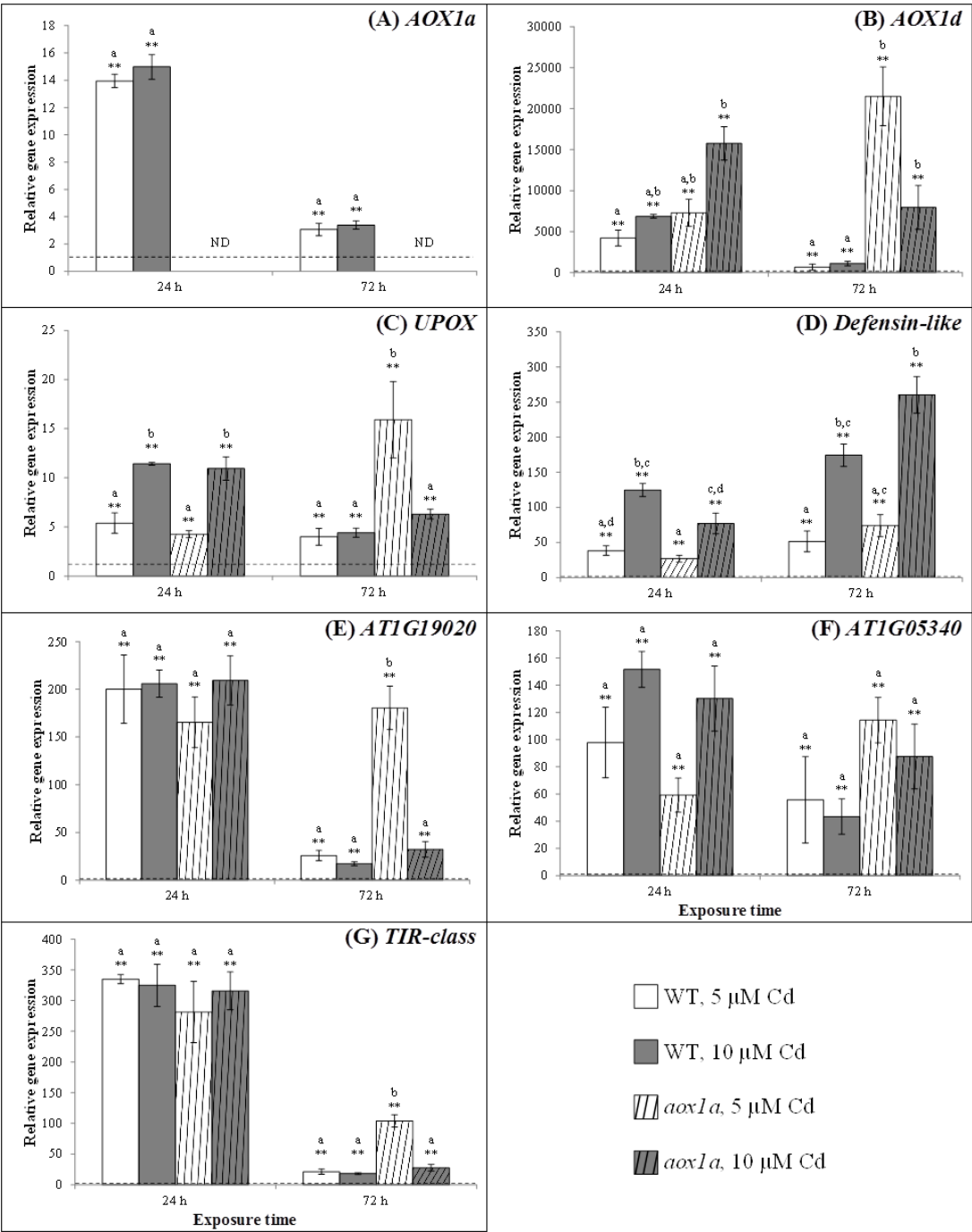


Fig. 2.



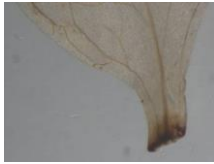









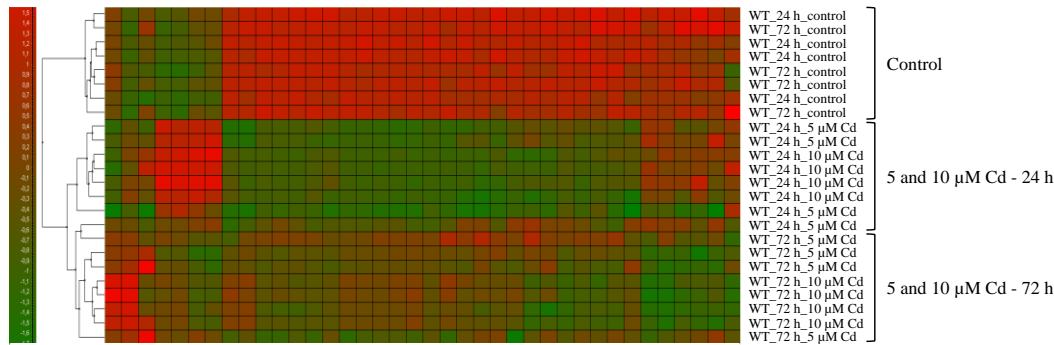
24 h				72 h			
WT		<i>aox1a</i>		WT		<i>aox1a</i>	
Control							Control
5 μ M Cd							5 μ M Cd
10 μ M Cd							10 μ M Cd

Fig. 3.

A



B

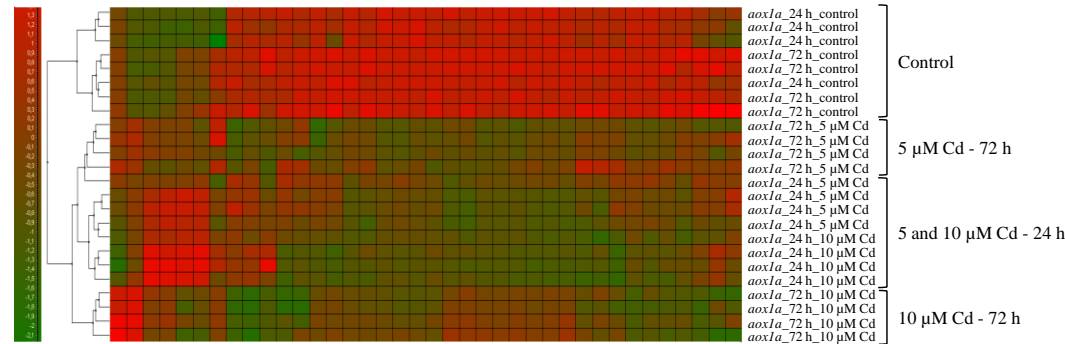


Fig. 4.

